Opening the KcsA K^+ Channel: Tryptophan Scanning and Complementation Analysis Lead to Mutants with Altered Gating†

Stacey N. Irizarry,‡ Esin Kutluay,‡,§ Gabriele Drews,‡ Sarah J. Hart,‡ and Lise Heginbotham*,‡

Department of Molecular Biophysics and Biochemistry, Yale University, New Haven, Connecticut 06520-8114, and Department of Biochemistry, Weill Graduate School of Medical Sciences, Cornell University, New York, New York 10021

Received July 2, 2002; Revised Manuscript Received August 19, 2002

ABSTRACT: The properties of the KcsA channel were investigated using a combination of tryptophan scanning of the two transmembrane helices followed by random mutagenesis at targeted residues. The tryptophan mutants were subjected to two screens: oligomeric stability and ability to complement the K^+ uptake deficiency of the TK2420 *Escherichia coli* strain. Oligomeric stability is affected primarily by mutations at sites that border on and interact with the selectivity filter, while the complementation assays identified residues at the crossing point of the inner helices. Sites identified by the complementation assay in the tryptophan screen were subjected to random mutagenesis and selection by complementation. We have found two mutants, A108S and A108T, which have dramatically increased open probability while retaining the basic property of oligomeric stability.

The KcsA potassium channel has proven extraordinarily accessible to biochemical studies. In addition to the high-resolution structures of the protein itself (*1*, *2*), crystallographic analysis has also allowed a molecular characterization of ion permeation (*3*). Given this extraordinary base of structural data, KcsA provides a unique opportunity to understand, at the molecular level, the functional properties of a gated, ion-selective channel.

Ironically, very little is known about the functional properties of KcsA. KcsA has proven a nearly intractable subject for traditional electrophysiological recordings. When reconstituted into planar lipid bilayers, KcsA is activated by protons on its cytoplasmic face (*4*, *5*). The acidic bath conditions necessary for proton activation preclude the use of MTS[1] reagents to map conformational changes associated with gating and thus rule out an approach that has proven particularly valuable in the related eukaryotic channels (*6*). Moreover, even at low pH, KcsA displays a low maximum open probability in physiological concentrations of K^+ (*4*). This has made detailed mechanistic studies with high-affinity inhibitors so far impossible.

To facilitate such studies, we sought to identify mutants that affected the gating of KcsA. We have used a combination of tryptophan scanning, random mutagenesis, and electrophysiological recordings to identify several point mutations of KcsA that dramatically increase the channel's open probability without affecting its tetrameric stability. We anticipate that these mutants will finally permit a broad range of functional experiments, useful both in studies of high-affinity inhibitors and in dissecting the kinetic mechanism of KcsA gating.

MATERIALS AND METHODS

Materials. Chemicals were of reagent grade or higher and were from Sigma-Aldrich (St. Louis, MO) unless otherwise noted. Dodecyl maltoside and CHAPS were purchased from Anatrace (Maumee, OH). MOPS was from American Bioanalytical (Natick, MA). KCl was obtained from Fluka (Milwaukee, WI), and KOH was from J. T. Baker Chemical Co. (Phillipsburg, NJ) (87.5% purity). Lipids, 1-palmitoyl-2-oleoylphosphatidylethanolamine (POPE) and phosphatidylglycerol (POPG), were from Avanti Polar Lipids (Alabaster, AL).

The JM-83 and XL-1 Blue *Escherichia coli* strains were purchased from ATCC (Manassas, VA) and Stratagene (La Jolla, CA), respectively, and the TK2420 strain was kindly provided by Wolf Epstein (University of Chicago). The JM-83 strain was grown in either Luria broth (LB, per liter: 10 g of tryptone, 5 g of yeast extract, and 10 g of NaCl), or Terrific broth (TB, per liter: 12 g of tryptone, 24 g of yeast extract, and 4 mL of glycerol, with 17 mM KH_2PO_4 and 72 mM K_2HPO_4). The TK2420 strain was grown in liquid culture in KLM (per liter: 10 g of tryptone, 5 g of yeast extract, and 10 g of KCl). TK2420 cells were plated on either LB plates or on solid media with defined concentrations of K^+. The plates contained a total of 115 mM combined K^+ and Na^+, made by combining the appropriate volumes of K115 and Na115 [X115: 46 mM X_2PO_4, 23 mM XH_2PO_4, 0.4 mM $MgSO_4$, 8 mM $(NH_4)_2SO_4$, 1 mM sodium citrate, 8 μM $FeSO_4$, 1 mg/L vitamin B_1, and 40% glucose].

Solutions used for planar lipid bilayer recordings are named according to the convention *n*K*m*, where *n* denotes

† L.H. is a Clare Booth Luce Assistant Professor and Pew Scholar in the Biomedical Sciences. E.K. has a Boehringer Ingelheim graduate fellowship. Support for this work was provided by a grant from the National Institutes of Health (GM41747) to L.H.

* To whom correspondence should be addressed. Tel: 203-432-9803. Fax: 203-432-5175. E-mail: Lise.Heginbotham@Yale.edu.

‡ Yale University.

§ Cornell University.

[1] Abbreviations: CHAPS, 3-[(3-cholamidopropyl)dimethylammonio]-1-propanesulfonate; Gly, glycine; MOPS, 3-morpholinopropanesulfonic acid; MTS, methanethiosulfonate; SDS, sodium dodecyl sulfate.

10.1021/bi026393r CCC: $22.00
Published on Web 10/23/2002

the concentration of K^+ ion (in millimolar) and *m* denotes the pH. 20K4 contained 16 mM KCl and 10 mM succinate; 20K5.5 contained 6 mM KCl and 10 mM succinate; 20K7 contained 16 mM KCl and 10 mM MOPS; 200K4 contained 196 mM KCl and 10 mM succinate; 200K5.5 contained 186 mM KCl and 10 mM succinate; 200K7 contained 196 mM KCl and 10 mM MOPS. The pH of all solutions was adjusted with KOH to provide the final indicated concentrations of K^+.

Anti-KcsA Antibody Preparation. Polyclonal anti-KcsA antibody was generated by immunizing rabbits with full-length KcsA protein (Cocalico Biologicals, Inc., Reamstown, PA). Anti-KcsA positive serum was harvested after a primary inoculation and two boosts. Anti-KcsA antibody was affinity purified by passing serum over a column containing immobilized KcsA (Bio-Gel; Bio-Rad, Hercules, CA) and eluting at low pH.

KcsA Construct and Mutagenesis. The KcsA construct serving as a template for all studies described here was as previously described (*7*). Briefly, the construct used a synthetic gene encoding the native protein sequence with addition of an N-terminal His_6 tag. This gene was inserted into the pASK90 expression plasmid (generously supplied by Dr. Arne Skerra); expression was induced by the addition of anhydrotetracycline (aTC; Acros Organics, Morris Plains, NJ). Site-specific mutants were generated with QuickChange mutagenesis (Stratagene, La Jolla, CA) and verified by sequencing of the entire KcsA coding sequence. In the case of A92W, the sole mutation that produced no protein, two independent colonies were checked to decrease the likelihood that lack of protein resulted from a stray mutation in the noncoding portion of the plasmid. Random mutagenesis at specific sites was carried out using QuickChange mutagenesis with primers degenerated at the targeted codon. XL-1 Blue *E. coli* were transformed with mutagenic plasmid and grown overnight in liquid culture. DNA was isolated from these bacteria and used to transform TK2420 *E. coli* for the screen.

SDS−PAGE. Typically, 0.5−2.0 μg of protein was loaded per well. Samples were loaded into a 4% stacking gel and separated on 15% gels using standard SDS−PAGE protocols.

Western Blots. For Western blotting, proteins were transferred from the separating gels onto nitrocellulose using a wet Western transfer protocol. Blots were blocked in 5% dry milk and incubated with 2.1 μg/mL rabbit anti-KcsA antibody, followed by 0.3 μL/ml goat anti-rabbit HRP (Bio-Rad). Signals were generated using the ECL plus reagent kit (Amersham Pharmacia, Piscataway, NJ) and detected using Kodak Bio-Max imaging film (Rochester, NY).

Testing Oligomeric Stability. JM-83 *E. coli* were transformed with plasmid DNA and grown overnight in liquid culture. Bacteria were then diluted in LB with ampicillin and allowed to grow to mid-log phase. Expression of KcsA protein was induced at $OD_{550} = 0.5$ by the addition of 200 μg/L anhydrotetracycline (aTC; Acros Chemical Co.) for 90 min. Cells were collected and solubilized in lysis buffer (6 M urea, 10 mM Na_2HPO_4, and 1% SDS, pH 7.2), and Laemmli sample buffer was added prior to running the samples on SDS−PAGE. Oligomeric stability was gauged by the presence of a band migrating at an anomalously high molecular mass on SDS−PAGE. We and others have previously shown that this band is comprised of tetrameric protein (*7*, *8*).

Complementation of TK2420. TK2420 *E. coli* were transformed with plasmid and grown overnight in a liquid culture of KML with ampicillin. The culture was diluted in KML with ampicillin and allowed to grow to mid-log phase ($OD_{550} = 0.5$); expression of KcsA protein was induced by the addition of 200 μg/L aTC. For the tryptophan screen, after 60 min of induction cultures were normalized by OD_{550}, and 3.5 μL drops of culture were spotted on LB plates, or 115K^+, 1K^+, and 0K^+ plates with ampicillin, with and without aTC. For selection of random mutants, cultures were plated after 60 min. Elemental analysis of the agar used (Element Analysis Corp., Lexington, KY) indicates that it adds an additional 1 mM K^+ to the K^+ concentration of the minimal media formulation (plates formulated with 0 mM K^+ media actually have 1 mM K^+). Plates were incubated at 37 °C until colonies formed. On plates containing low and no aTC, incubation times ranged up to 4 days.

KcsA Purification and Reconstitution. The wild-type and mutant KcsA proteins were expressed and purified as previously described (*5*, *9*). Briefly, after induction, cells were washed and resuspended in buffer A (95 mM NaCl, 5 mM KCl, and 50 mM MOPS, adjusted to pH 7.0 with NaOH), protease inhibitors (final concentrations: leupeptin, 1 μM; pepstatin A, 1 μM; PMSF, 0.5 mM) were added, and cells were disrupted by a French press. Unbroken cells were cleared by centrifugation at 12000*g* for 25 min, and membranes were isolated by ultracentrifugation at 75000*g* for 45 min. Membranes were resuspended in buffer B (95 mM NaOH and 5 mM KCl, pH 7.0, with H_3PO_4) and extracted using 15 mM dodecyl maltoside for 30 min. Protein was purified using nickel affinity chromatography (Ni-NTA Agarose, Qiagen) and eluted with 400 mM imidazole. Purified KcsA was immediately reconstituted into lipid micelles as described previously (*5*, *9*).

Single Channel Recordings in Lipid Bilayers. Single channel recordings were performed in a horizontal planar lipid bilayer setup. Briefly, partitions made from overhead transparency film having holes of roughly 50 μM in diameter were pretreated by application of ~0.2 μL of lipid solution (15 mg/mL POPE + 5.0 mg/mL POPG in decane) to the hole, followed by 20 min of drying in air. After the chambers were filled with solution, bilayers were formed by painting with a glass rod dipped in the lipid solution. Sample was added to the *cis* chamber, and the bilayer was formed with the bubble expelled by the pipet after the addition of sample.

The orientation of the recording system is such that the *cis* chamber, containing 200 mM K^+ solutions at pH 7, is equivalent to the periplasmic surface of the protein, while the intracellular surface of the channel faces the *trans* chamber. Voltages and currents follow the standard electrophysiological convention, with extracellular solution at ground voltage. Current was sampled at 10 kHz and low-pass filtered at 2 kHz.

Data were acquired and analyzed with Clampex and P-stat software (Axon Instruments). Long closed times (>100 ms) were included in the determination of P_o, but their rare occurrences precluded our fitting them during analysis of mean closed times. Dwell time distributions were fit with exponential components using least-squares fitting. For the wild-type channel, open time histograms were fit with two exponentials while closed time histograms were fit with three; inclusion of additional exponential components did not

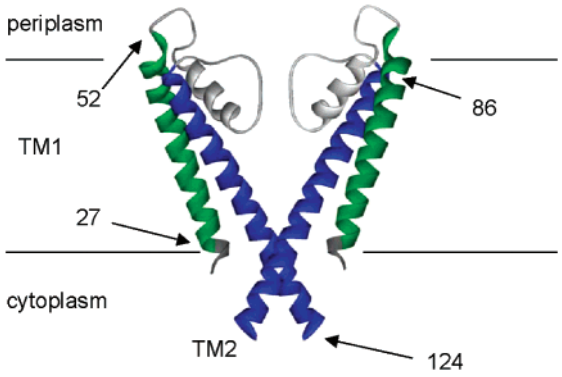

FIGURE 1: Segments of the KcsA channel targeted by mutagenesis. The transmembrane portion of two of the four subunits of the KcsA channel is shown with a ribbon diagram. Horizontal lines define the expected general position of the lipid bilayer. The selectivity filter, pore helix, and adjacent loops are colored light gray. The transmembrane segments targeted for scanning mutagenesis are indicated in green for the outer helix (TM1) and in blue for the inner helix (TM2). Our scan extended beyond TM2 to residue 128; the final four residues are not ordered in the 1K4C crystal structure. The dark gray residues (24−26) were not targeted in this study. This figure was generated from PDB file 1K4C using WebLab ViewerPro (Molecular Simulations Inc., Cambridge, U.K.).

appreciably improve the fit. Initial analysis of histograms for the A108S and A108T mutant channels was done similarly. This was subsequently modified by using two component fits for the closed time histograms, as addition of a third component did not improve the fit. The closed times for A108S and A108T shown in Table 3 were derived from two component fits.

RESULTS

Target Regions and Strategy. The objective of this study was to identify mutations that increased the open probability of KcsA. The high-resolution structure of KcsA, as well as functional data from the related voltage-activated K^+ channels, guided the selection of targets in our initial scanning mutagenesis.

KcsA is a homotetrameric protein, with each subunit containing two complete transmembrane spanning helices in addition to a third, shorter pore helix that positions the selectivity filter (Figure 1) (*1*). Comparisons of the potassium channel crystal structures with functional data from the K_v channels indicate that gating involves a conformational rearrangement of at least the cytoplasmic end of the inner helix (*10*−*12*). As mutations of the selectivity filter, pore helix, and surrounding loops can have dramatic effects on both ionic selectivity and protein stability (*7*, *13*, *14*), we limited our focus to the two transmembrane helices of KcsA.

We launched our search with a tryptophan scan, probing from position 28 to position 52 on TM1 and from position 86 to position 128 on TM2 (Figure 1). At sites where the native residue is tryptophan, we sequentially substituted alanine to maximally perturb side chain volume while minimizing any effect on backbone conformation. Each tryptophan mutant channel was evaluated for changes in function and stability. We then targeted a small group of sites identified by the scan for more detailed analysis using random mutagenesis and electrophysiological recordings.

Oligomerization. To be useful in bilayer experiments, a mutant channel must be sufficiently robust to endure the purification process. Empirically, there appears to be a tight correlation between mutants that withstand purification in mild detergents and those that maintain their tetrameric architecture in much harsher SDS micelles (E. Kutluay and L. Heginbotham, unpublished observation). Since the oligomerization state in SDS is easily assayed with SDS−PAGE (*7*, *8*), we used this technique to screen the entire panel of tryptophan mutants.

The Coomassie-stained gel in Figure 2A illustrates the basic assay: although heat-denatured KcsA migrates as predicted by molecular mass (lane 1), the bulk of the original purified sample migrates much more slowly (lane 2). We and others have shown that the high molecular mass species is tetrameric KcsA migrating at an anomalous position (*7*, *8*); since the tetrameric species is disrupted by conservative mutations adjacent to the selectivity filter (*7*), it appears to be at least partially folded.

We used Western blots to assay KcsA mutants directly from total cellular lysates. This approach avoids several potential difficulties, for instance, if the mutations greatly reduce the yield upon purification, either by reducing the quantity of induced protein or by altering the accessibility of the tag used in purification. Like the Coomassie-stained gels of purified protein, Western blots of purified KcsA show little monomeric species unless the protein is subjected to heat denaturation (Figure 2B, lanes 1 and 2). In contrast, total cellular lysate shows a strong signal from a low molecular mass protein even before denaturation (Figure 2B, lanes 3 and 4). The low molecular mass protein is induced KcsA protein, since it is not evident in lysates from mock-induced JM-83 cells (Figure 2B, lane 5), and in fact appears to be incorrectly folded protein located in inclusion bodies (data not shown). Because of the presence of monomeric KcsA species in the whole cell lysates, we have limited our analysis to the simple question: how does tryptophan mutagenesis affect the presence of tetrameric protein?

Most of the tryptophan mutants retained a tetrameric architecture upon SDS−PAGE, indicating that oligomerization was largely unaltered by tryptophan substitution. V91W, V93W, V94W, and V97W are typical of these mutant channels and show the same pattern of expression as the wild-type channel (Figure 2C, lanes 1, 2, 4, 5, and 8). In some cases, as illustrated by V93W and V94W, the ratio of tetramer to monomer appears to be higher than that of the wild-type channel, suggesting that some mutations may actually *increase* stability.

In contrast, 10 tryptophan mutants yielded little or no detectable tetrameric species (Table 1). However, as illustrated with V95W and M96W, most of these mutants did yield substantial quantities of monomeric protein (Figure 2C, lanes 6 and 7). Preliminary studies indicate that, with the exception of A47W, each of these mutant proteins is found in the membrane fraction. If so, then the primary effect of these mutations may be a decrease of oligomeric stability in SDS rather than a disruption of folding or membrane insertion.

A single mutant, A92W, failed to yield detectable levels of protein (Figure 2C, lane 3). This may result from altered RNA stability, altered protein stability, or decreased protein synthesis; we have not studied this mutant further.

The sites at which tryptophan substitution disrupts tetramerization are found on both TM1 and TM2. A clear

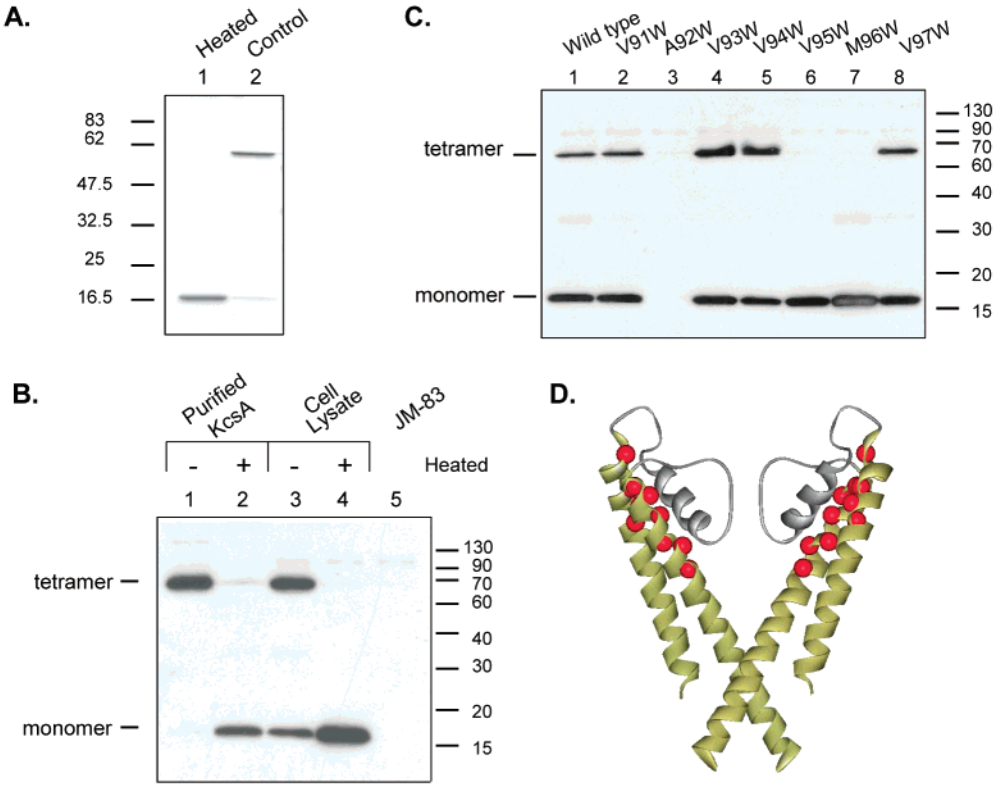

FIGURE 2: Oligomeric stability of the tryptophan mutant channels. Samples were separated on a 15% gel using SDS−PAGE and visualized either with Coomassie blue stain (A) or using immunodetection after transferring to nitrocellulose (B and C). (A) Purified KcsA protein run before (lane 2) and after (lane 1) heating to 95 °C for 10 min. (B) Western blots of purified KcsA protein look similar to Coomassie stained gels (lanes 1 and 2), while total cellular lysate from *E. coli* expressing KcsA protein displays monomeric protein even prior to heat treatment (lanes 3 and 4). The polyclonal antibody does not react with any endogenous proteins from the host JM-83 *E. coli* strain that migrate at the position of either tetrameric or monomeric KcsA (lane 5). (C) Western blot of cellular lysates from *E. coli* expressing wild-type KcsA (lane 1) and the tryptophan mutant channels from position 91 through 97 (lanes 2−8). (D) Red spheres indicate the locations of the α carbons on residues disrupting oligmerization (G43, S44, A47, E51, G88, R89, A92, V95, M96, G99) superimposed on the KcsA structure. The picture of two of the four subunits was made as described in the legend to Figure 1.

Table 1: Summary of the Results of the Tryptophan Scan[a]

assay	sites identified
oligomerization	G43, S44, A47, E51, G88, R89, A92, V95, M96, G99
complementation	A108, A109, A111, T112

[a] Mutants which disrupt tetramerization as assayed using SDS−PAGE, or which complement the phenotype of the TK2420 strain, are indicated. (For comparison, wild-type KcsA displays oligomers on SDS−PAGE and does not complement the phenotype of the TK2420 strain.)

picture of why these mutations affect tetramerization emerges when our data are compared with the crystal structure of KcsA. As shown by the overlay of our data with the KcsA structure (Figure 2D), these sites are all located on the outer part of the protein. Half of the residues are located at the interface of the transmembrane helices. Nearly every residue directly contacts the pore helix or the loops on either side of the selectivity filter, thereby lining a nest that cradles the selectivity filter. The two exceptions, E51 and G88, are located at the top of the outer and inner helix, respectively, and are in direct contact with one another. Intriguingly, it is precisely this upper half of the membrane core that appears relatively immobile during the conformational changes associated with gating (see Discussion).

The oligomerization assay provides a criterion for use in evaluating which mutants are ultimately biochemically suitable for reconstitution into planar lipid bilayers. We next focused on identifying mutations that have effects on channel function.

Complementation of TK2420. When functional ion channels are expressed in the plasma membrane, their activity can have profound consequences for the viability of the host cell. In such cases, complementation assays can be used to identify clones with altered channel function. Genetic screens, by nature, isolate a number of complementation groups that complement the phenotype through different mechanisms. However, the use of such screens is a powerful means of isolating potentially interesting mutants. This approach has proven utility: the *Arabidopsis* potassium channels Kat1 and AKT1 were originally expression cloned through their complementation of yeast strains deficient in K^+ uptake (*15*, *16*), and gating mutants of MscL, the mechano-sensitive channel from *E. coli*, have been isolated through their effects on *E. coli* growth (*17*−*19*). Moreover, numerous studies have used complementation of yeast strains deficient in K^+ uptake to examine the functional properties of eukaryotic potassium channels (*20*−*23*); several of these have isolated gating mutants (*20*, *22*, *23*).

To select for KcsA mutants with altered activity, we used a host strain of *E. coli* deficient in K^+ uptake whose phenotype is not complemented by expression of the wild-type KcsA channel. In wild-type *E. coli*, K^+ uptake is mediated by three major systems: Kup, Trk, and Kdp. The

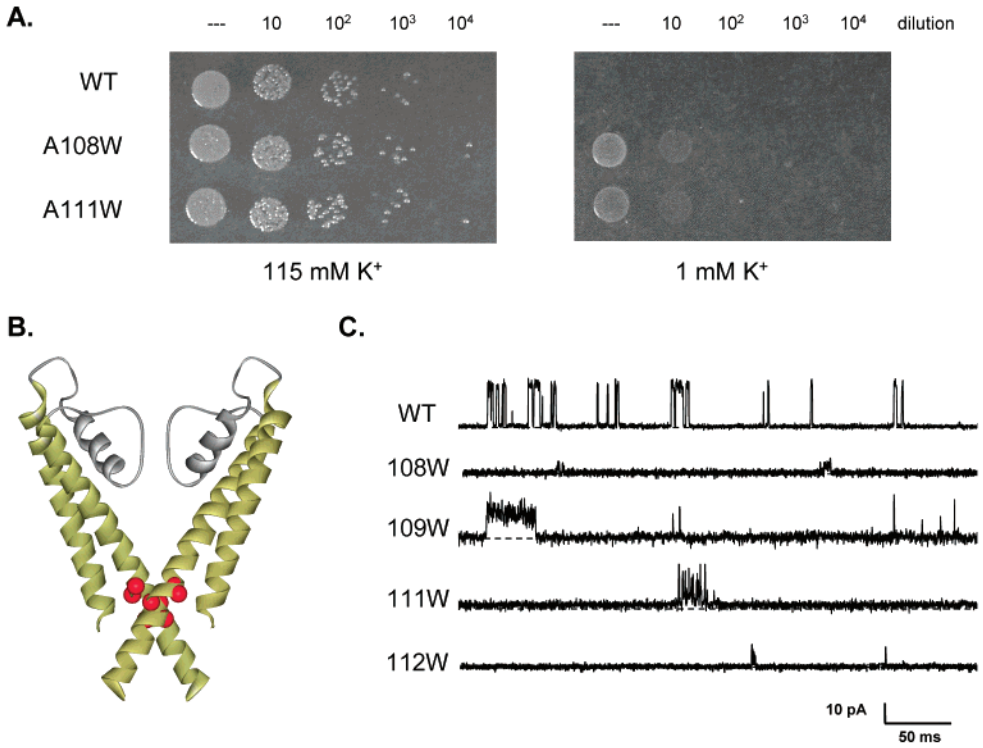

FIGURE 3: Complementation of the TK2420 *E. coli* strain by tryptophan mutant channels. (A) TK2420 *E. coli* containing plasmid encoding the wild-type KcsA channel or either the A108W or A111W mutant channels was grown to mid-log phase in KML, expression of the mutant channel was induced by addition of 0.2 mg/mL aTC for 60 min, and cells were resuspended at an OD_{600} of 0.3. The 3.5 μL aliquots of the cell suspension were plated in serial dilutions (dilutions indicated on the top of the figure) on 115 mM K^+ plates or 1 mM K^+ plates. Plates were incubated at 37 °C overnight (115 mM K^+) or for 3 days (1 mM K^+) prior to photography. (B) Red spheres indicate the locations of the α carbons on residues complementing the TK2420 strain (A108, A109, A111, T112) superimposed on the KcsA structure. The picture of two of the four subunits was made as described in the legend to Figure 1. (C) Currents through single mutant KcsA channels. Recordings were made from the indicated mutant channels at 200 mV in 200K7/200K4 solutions (except A108W, which was recorded in 200K7/20K4). Dashed lines indicated the closed state.

TK2420 *E. coli* strain is deficient in each of these pathways and requires K^+ supplementation for growth (*24*). Induction of the wild-type KcsA protein is insufficient to complement growth in low potassium (Figure 3A). This is not surprising, given the rare activity of KcsA under the salt and pH conditions expected in *E. coli* (*4*, *5*, *9*). The TK2420 strain therefore provides a suitable background for identifying gain of function mutants.

We screened the entire panel of tryptophan mutants using the TK2420 strain. Some of the tryptophan mutants, including A108W and A111W, did complement this phenotype and supported growth on plates containing low K^+ (Figure 3A). Four sites were identified by the screen (Table 1); they are all found in a single location, near the bundle crossing of the inner helix (Figure 3B). These sites are physically distinct from the group of residues that disturb oligomerization.

There are several different mechanisms by which a gain-of-function mutant might be expected to complement a potassium uptake deficiency. In addition to mutants that simply increase the open probability, mutants might also increase the conductance of the open state, or uncouple the gating mechanism, either by removing proton activation or by allowing ion permeation through the "closed" state. To learn if any of the mutants identified by the complementation assay had an increased P_o, we purified each and screened its behavior in planar lipid bilayers.

The mutant channels were studied under the conditions typically used in studies of wild-type KcsA (Figure 3C). Each of these tryptophan mutant channels behaved quite differently from the wild-type protein, but none had clearly increased P_o. Both A111W and A112W had infrequent openings of very brief duration (Figure 3C). As shown in Figure 3C, the A109W mutant channel did occasionally display a longer lived open state, but this state occurred rarely. The A108W mutant channel was even more dramatically affected. It was only active when the internal solution contained low internal K^+ (Figure 3C). The wild-type KcsA protein displays a similar salt sensitivity, with activity decreasing as the salt concentration rises (*9*), but the phenotype is more pronounced in the A108W mutant channel. We have not ruled out the possibility that these channels have modest changes in pH sensitivity, but preliminary studies indicate that they are not active in solutions with internal pH 7.

Because these particular mutant channels do not have clearly increased P_o, we have not characterized their behaviors extensively and do not know precisely the means by which they complement the TK2420 phenotype. It is possible that the tryptophan mutant channels are either constitutively leaky or have a very long lived small subconductance state; either would be undetectable with our bilayer recordings. It is also possible that the activity we record at room temperature in the bilayer setup does not accurately reflect activity in the intact *E. coli* at 37 °C.

Although the tryptophan scan did not reveal any mutants with increased open probability, it did point to the critical importance of four particular residues. The general location of these sites was promising, since these are precisely the

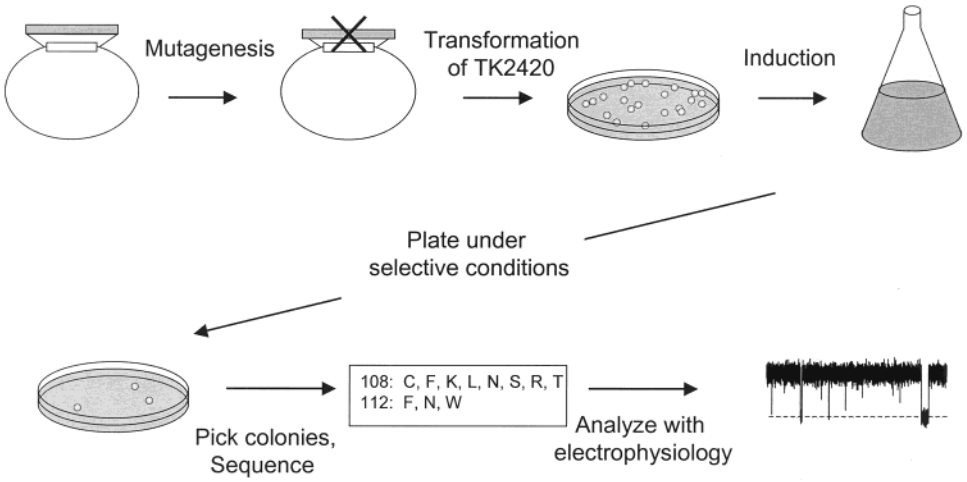

FIGURE 4: Schematic diagram of the approach used in random mutagenesis at targeted sites. Specific residues were targeted for random mutagenesis using the Stratagene QuickChange kit with oligonucleotides that contained a degenerate codon. Mutant plasmid was passaged through the XL-1 Blue strain once. TK2420 *E. coli* were transformed with this library and grown to mid-log phase; protein expression was induced by the addition of aTC and then plated under selective conditions. Individual colonies were picked, the plasmid DNA sequenced revealing the indicated mutants, and mutants were then studied using electrophysiological techniques.

residues that form a constriction at the cytoplasmic end of the pore in the KcsA structure (*1*), gating clearly involves movement of the protein in this region (*10*, *12*), and mutations of analogous residues in other channels are known to alter channel gating (*20*, *23*, *25*, *26*). We therefore decided to investigate whether less dramatic mutations at these four sites might have the desired properties.

Targeting the Complementing Residues. We used the TK2420 complementation assay to isolate additional mutants with altered phenotypes. We sequentially generated libraries of DNA with randomized codons at positions A108, A109, A111, and T112 and used the TK2420 strain to screen for mutants that complemented the low K^+ growth phenotype (Figure 4). To date, we have isolated a number of mutants from positions A108 and T112 (Figure 4); these represent our first attempts at screening these positions, and we have not yet quantitatively compared the relative abilities of the different mutants to complement the TK2420 phenotype. We tested each of these mutants and have confirmed that they retain the basic characteristic of oligomeric stability on SDS−PAGE and thus were good candidates for subsequent studies requiring purification. The blots of cellular lysate from two of these mutant proteins, clearly showing that both A108S and A108T generate stable tetrameric species, are illustrated in Figure 5A.

We purified protein and checked many of these channels after reconstitution into planar lipid bilayers. Most of the channels, like the tryptophan mutants at these positions, show either wild-type behavior or less activity than wild type. However, two of the mutant channels, A108T and A108S, display gating behaviors clearly consistent with our original expectation that the screen would identify a class of channel with increased open probability.

The A108S and A108T mutant channels both have altered gating characteristics (Figure 5B,C). The characteristic bursting behavior of these mutants is illustrated in a record from a bilayer containing a single A108T channel in Figure 5B. Here, frequent periods of rapid openings and closings are interspersed with longer silent events of roughly 5 s in duration, creating a bursting pattern to the observed activity.

The two mutant channels have much higher open probabilities (P_o) than that of the wild type (Figure 6A, all-points histograms; Table 2). In internal solutions containing 200 mM K^+ at pH 4, the P_o of these mutant channels is roughly 20% for A108T and 30% for A108S (Table 2). Although the P_o of the mutant channels can be determined with reasonable accuracy, our value of P_o (3%, Table 2) for the wild-type channel is certainly an overestimation, since at such low open probabilities it is difficult to ascertain the true number of channels in the bilayer. Thus, the P_o of the A108S mutant channel is *at least* 10-fold greater than that of the wild type under these same conditions (Table 2).

We investigated the kinetic properties of these two mutant channels to examine the origin of the increased open probability. Analysis of our data reveals that both open and closed dwell times are comprised of multiple kinetic components. The primary effect of both the A108S and A108T mutations is to eliminate the most prevalent, and longest, closed state observed in the wild-type channel (τ_3, Table 3). The distribution of the remaining closed states is also altered, with τ_1 now being the major component (Table 3). This destabilization of the closed state is sufficient to account for the increased open probability seen in the A108T mutant channel. The A108S mutation additionally stabilizes the open state by extending the duration of the longest dwell time (τ_2, Table 3), as well as increasing its prevalence.

KcsA activity is sensitive to ionic conditions; the channel is activated by protons from the intracellular side and is inhibited by high ionic strength (*4*, *5*, *9*). We have examined both effects in the A108T and A108S mutant channels (Table 3). The mutants retain their basic sensitivity to internal pH; changing the internal solution from pH 4 to pH 5.5 decreases P_o (Table 3), and no activity was observed when the internal solution was buffered at pH 7.

In contrast, the two point mutations have a dramatic effect on the sensitivity of the channel to ionic strength (Table 2). In most potassium channels, gating is known to be coupled to permeation, since closing rates are slower in Rb^+ than K^+. This is traditionally explained by a foot-in-the-door model, in which a channel cannot close if a specific site

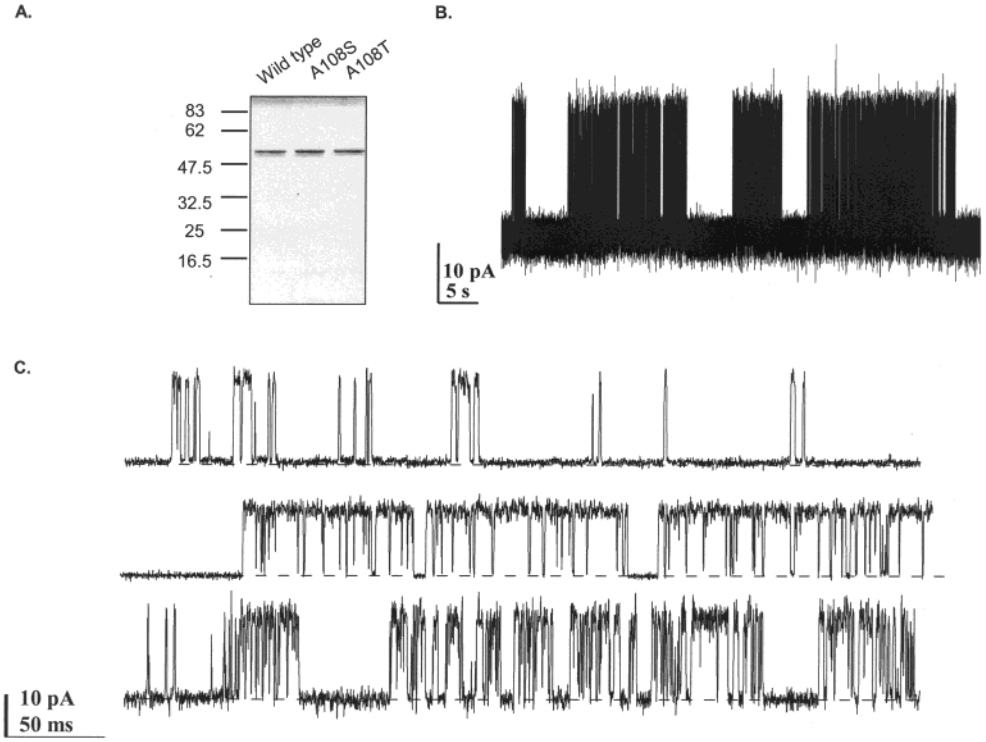

FIGURE 5: Mutants of KcsA increase the channel open probability. (A) Oligomeric stability of wild-type KcsA and the A108S and A108T mutant channels. Both mutants form stable tetrameric species as evidenced by their migration pattern on SDS−PAGE. (B) A108T channels show bursts of activity. Shown is a single channel record made at 200 mV with 200K4 internal solution, illustrating the typical bursting behavior of the mutant channel. (C) Comparison of wild-type KcsA with A108S and A108T. WT KcsA (top trace) enters a longer lived closed state than A108S (middle trace) or A108T (bottom trace) during a typical burst period. All recordings were made at 200 mV with 200K4 internal solution and were low-pass filtered at 2 kHz.

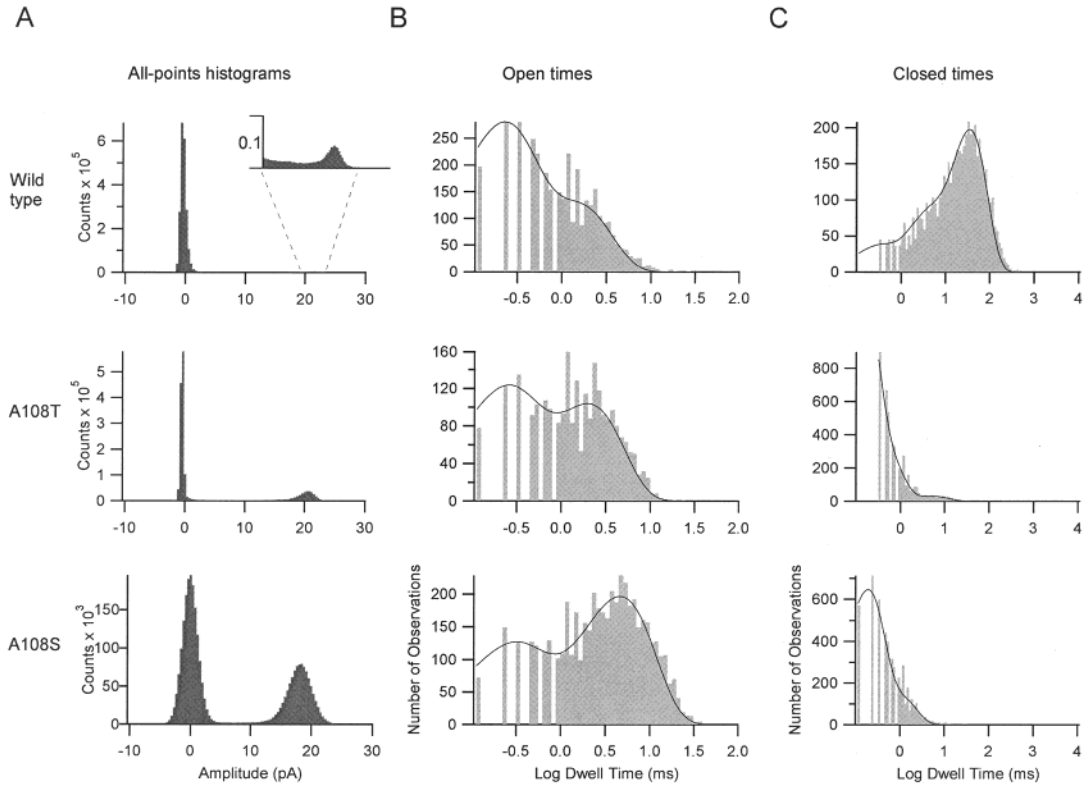

FIGURE 6: Representative illustrations of all-points histograms (A), mean open times (B), and mean closed times (C) for wild-type KcsA (top row), A108T (middle row), and A108S (bottom row). Axis labels for each set of graphs are given on the last graph in the column. The inset in the histogram for the wild-type channel illustrates the paucity of open events. Dashed lines represent exponential fits to the data (B and C). The number of binned events for each dwell time distribution was at least 5000. Data were recorded in internal 200K4 at +200 mV.

within the pore contains a permeant ion (*27*, *28*); Rb^+ binds more tightly than K^+ and therefore slows the kinetics. Wild-type KcsA protein actually displays a behavior that is inconsistent with this model, since it has higher P_o at low

Table 2: Open Probability of Wild-Type and Mutant Channels under Differing Salt and pH Conditions in the Internal Solution[a]

	WT	A108T	A108S
20 mM K^+, pH 4.0	0.07 ± 0.02	0.16 ± 0.04	0.15 ± 0.02
20 mM K^+, pH 5.5	0.017 ± 0.016	0.16 ± 0.06	0.10 ± 0.02
20 mM K^+, pH 7.0	undetected	undetected	undetected
200 mM K^+, pH 4.0	0.03 ± 0.01	0.20 ± 0.06	0.30 ± 0.03
200 mM K^+, pH 5.5	undetected	undetected	undetected
200 mM K^+, pH 7.0	undetected	undetected	undetected

[a] External solution in all the cases was 200K7. $n \geq 3$ for all data. Channel open probabilities were calculated from Gaussian fits to all-points histograms (Figure 6A). Values are expressed as mean ± SEM. Undetected refers to records where no activity was apparent. Because the open probability of the wild-type channel is so low in 200K4, we were unable to ascertain that there was in fact only a single channel in the bilayer. Thus the P_o value stated here of 0.03 serves as an upper estimate of the true open probability under these conditions.

Table 3: Dwell Times for Open and Closed States of WT, A108T, and A108S KcsA[a]

		WT	A108T	A108S
open times	τ_1	0.20 ± 0.01 (0.72)	0.25 ± 0.03 (0.67)	0.22 ± 0.01 (0.48)
	τ_2	1.14 ± 0.09 (0.28)	2.60 ± 1.40 (0.25)	4.36 ± 1.60 (0.52)
closed times	τ_1	0.43 ± 0.09 (0.19)	0.47 ± 0.14 (0.84)	0.48 ± 0.20 (0.79)
	τ_2	4.23 ± 1.10 (0.30)	5.40 ± 1.50 (0.16)	1.48 ± 0.43 (0.25)
	τ_3	29.2 ± 5.30 (0.65)		

[a] All values reported are for recordings made with 200K4 internal solution. Mean open and closed times were calculated from least-squares fits to log dwell time distributions (Figure 6B,C). Open and closed times (τ) are given in milliseconds as mean ± SEM. The proportion of each time constant is given in parentheses. n = six to eight measurements for all three channels.

salt concentrations. [KcsA is not unique in this regard; $K_{ir}1.2$ has the same phenotype (*29*).] The A108S and A108T mutant channels actually reverse the sensitivity of the wild-type channel so that their activity increases at high salt concentrations. It is possible that the longest kinetic component of the wild-type channel, τ_3, reflects a closed state that is particularly stabilized by internal potassium and which is not entered when mutations are made at position A108.

DISCUSSION

KcsA has proven remarkably amenable to structural studies using crystallographic techniques. Although several detailed studies of the permeation properties of the channel exist, the gating properties of this channel have prevented many experiments that would permit both direct comparisons of gating with eukaryotic channels and mechanistic studies with high-affinity blockers. The chief obstacle to such studies is the extremely low maximal open probability of the wild-type channel at physiological salt concentrations. We therefore sought to identify mutants of the channel that had increased open probability.

Recently, tryptophan scanning has enjoyed wide use in evaluating helical packing models of eukaryotic channels (*30*−*33*). In each application, some of the resulting tryptophan mutant channels have had dramatically altered gating characteristics. We suspected that an analogous scan of the KcsA channel might generate similar mutants.

We deliberately used two very different screens to scan a broad target group. The first criterion, evaluated through the SDS−PAGE oligomerization assay, was that the mutants be biochemically stable. Stability is particularly critical since KcsA is studied after detergent solubilization and reconstitution, in contrast to eukaryotic channels that are typically examined in intact cellular membranes. A second complementation screen was used to identify gain-of-function mutations; this screen exposed the critical importance of four positions. In electrophysiological recordings, these four tryptophan mutant channels are not obviously open more than the wild-type channel, and the precise mechanism by which they achieve complementation remains unclear. However, further random mutagenesis at these four sites did generate several mutants with dramatically increased P_o.

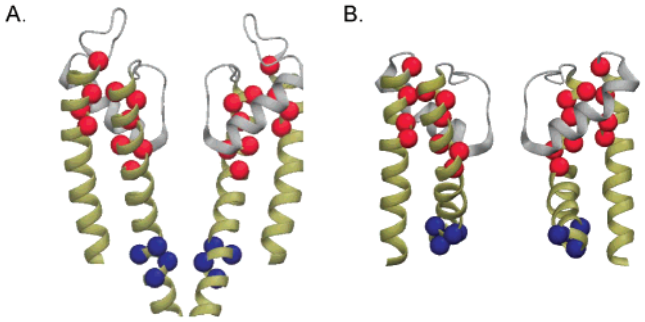

FIGURE 7: Positions of the sites identified by the oligomerization and complementation screen overlayed on the structures of KcsA (A) and MthK (B). Red and blue spheres indicate the positions of α carbons on residues that were identified by oligomerization and complementation assays, respectively. The channels illustrated here are rotated roughly 30° around the axis of symmetry as compared to those in Figures 2 and 3. This figure was drawn using DINO from PDB files 1K4C (truncated at residue 118) and 1LNQ (A. Philippsen).

Results of Screens. Although we have used the KcsA crystal structure to display the locations of residues identified in our screens, analysis of our data is further aided by examining the sites of analogous residues in the MthK structure (*34*). The MthK potassium channel, from the bacterium *Methanobacterium thermoautotrophicum*, has a membrane topology similar to that of KcsA, and the two channels display sufficient homology to permit alignments of the transmembrane domains. The KcsA and MthK structures are thought to reflect the closed and open states of potassium channel pores, respectively (*12*), and a glycine residue proposed to be critical for the gating transition is conserved. The primary difference in the two structures is at the inner entryway to the pore. In the closed KcsA structure, the inner helices are relatively straight and meet in a bundle at the cytoplasmic end. In contrast, there is a kink approximately midway through the MthK inner helix. Located at a glycine residue, the kink redirects the inner helix, resulting in a broadening of the pore at the cytoplasmic face.

Our scans of the KcsA transmembrane helices highlight the importance of two tightly clustered groups of residues (Figure 7). Residues where tryptophan mutation decreases oligomeric stability are primarily located at the interface of the P-region and the transmembrane helices, lining a nest for the selectivity filter and adjacent structures. As expected, our screen identified a region in which the protein is tightly packed; not surprisingly, the architecture in this region is quite conserved between KcsA and MthK. In contrast, tryptophan substitution along the cytoplasmic ends of the helices had no impact on tetramer stability. This is easily

understood in light of the crystal structures, since these segments must be flexible in order to accommodate the large, proposed movements during gating (*12*). Our work indicates that there are two distinct environments, where tetramerization of the channel is sensitive or insensitive to tryptophan substitution, and that the transition point between them is sharp. The last residue at which tryptophan substitution affects tetramerization is Gly 99, the conserved glycine at which the inner helix is kinked in the open channel MthK structure (*12*).

Intriguingly, mutants identified by the complementation screen were located in a single location near the C-terminus of the inner helix. We anticipated that mutations at this location might effect complementation; mutagenesis, chimera, and complementation studies of several eukaryotic channels (*20*−*23*, *25*, *26*, *35*) illustrate the importance of this region in gating, and the complementation assay selects for channels with altered functional properties. In contrast to the residues that affected oligomerization, these sites do change disposition during gating (*12*). In the closed channel structure of KcsA, these residues are located at the bundle crossing of the inner helices whereas, in the MthK structure, the movement of the inner helix repositions them away from the central axis of the conduction pore.

In the absence of crystal structures for most membrane proteins, investigators have frequently resorted to perturbation analysis (PA) to glean structural constraints for models of helical packing (*26*, *30*−*33*, *36*, *37*). Typically, tightly packed regions are located by identifying sites where nonconservative substitutions alter protein function. Although our screens differ from the standard electrophysiological studies typically used with PA, they provide the first opportunity to directly examine the utility of this approach. In general, PA worked remarkably well on KcsA; all residues identified by the screens were in fact located at a packed interface in the KcsA crystal structure. However, our screens missed identifying many interfaces, both inter- and intrasubunit, between the transmembrane helices themselves. We suspect this is simply a consequence of the flexibility inherent in these regions.

Mutations That Affect Gating. Through random mutagenesis at the sites originally identified through the tryptophan screen, we identified several mutants of KcsA that have greatly increased P_o compared with the wild-type channel. Because we have not fully saturated the screen, it is unclear precisely how mutations at A108 decrease closed state stability. We note, however, that it cannot be simply through bulk, since the A108W mutation does not appear to increase channel P_o. We do not yet understand precisely how the A108W mutant effects complementation, but we suspect it may be the result of increased permeability of the closed state.

The primary effect of these mutations was to decrease the stability of the closed state. In the high-resolution structure of KcsA, the A108 side chain makes direct contact with the adjacent helix, abutting residues T107 and A111. Given this packing arrangement, the introduction of four more hydroxyl groups by either serine or threonine substitution could have dramatic effects on closed state stability. The MthK structure is at lower resolution, and so the precise disposition of the equivalent side chain remains unknown. However, it is clear that the side chain faces entirely different environments in the open and closed states, and it is easy to understand how the stability of the closed state could be preferentially affected by mutation.

The A108T mutant channel shows distinctly altered K^+ dependence. This mutant offers an opportunity to study whether mutations in this region affect the activation gate per se or the coupling between the potassium sensor and channel gate. Similar studies are being conducted in voltage-activated K^+ channels, and it will be intriguing to see the extent to which the mechanisms of activation are conserved between this very minimal K^+ channel and its complex relatives.

Although our complementation assay identified a very localized set of residues, we suspect that mutations at many other positions also affect the functional properties of KcsA. It is intriguing, for example, that we have not yet isolated any mutants that stabilize the open state. We suspect, given the structure of the MthK channel, that such mutants will be located near the Gly 99 hinge. We are currently investigating whether more subtle mutations in this region affect gating. However, if the consequences of mutation at this site are sufficiently severe, it is possible that the mutant channels would remain undetected by our complementation screen. For example, channels that are nonspecifically leaky might kill rather than complement the phenotype of the TK2420 strain. Reprobing this area with a smaller perturbation (a residue other than tryptophan) may reveal other sites that affect gating.

Our identification of A108T and A108S using the complementation assay confirms its ultimate utility in identifying gating mutants. Our screen of the four sites identified by the initial tryptophan scan has not reached saturation, and we anticipate that continued use of this screen will yield channels with a variety of alterations in gating behavior. Already, however, the A108S and A108T mutant channels have sufficiently altered open probability to finally enable a wide variety of functional studies: from a kinetic characterization of the closed state to mechanistic studies of high-affinity blockers.

ACKNOWLEDGMENT

We thank W. Epstein for the generous gift of the TK2420 *E. coli* strain, Kyle Friend for preliminary experiments, J. Morais-Cabral, D. Engelman, M. Maduke, and C. Miller for helpful discussions, and C. Miller, J. Morais-Cabral, and F. Sigworth for helpful comments on the manuscript.

REFERENCES

1. Doyle, D. A., Morais Cabral, J., Pfuetzner, R. A., Kuo, A., Gulbis, J. M., Cohen, S. L., Chait, B. T., and MacKinnon, R. (1998) *Science 280*, 69−77.
2. Zhou, Y., Morais-Cabral, J. H., Kaufman, A., and MacKinnon, R. (2001) *Nature 414*, 43−48.
3. Morais-Cabral, J. H., Zhou, Y., and MacKinnon, R. (2001) *Nature 414*, 37−42.
4. Cuello, L. G., Romero, J. G., Cortes, D. M., and Perozo, E. (1998) *Biochemistry 37*, 3229−3236.
5. Heginbotham, L., LeMasurier, M., Kolmakova-Partensky, L., and Miller, C. (1999) *J. Gen. Physiol. 114*, 551−560.
6. Liu, Y., Holmgren, M., Jurman, M. E., and Yellen, G. (1997) *Neuron 19*, 175−184.
7. Heginbotham, L., Odessey, E., and Miller, C. (1997) *Biochemistry 36*, 10335−10342.

8. Cortes, D. M., and Perozo, E. (1997) *Biochemistry 36*, 10343−10352.
9. LeMasurier, M., Heginbotham, L., and Miller, C. (2001) *J. Gen. Physiol. 118*, 303−314.
10. Yellen, G. (1998) *Q. Rev. Biophys. 31*, 239−295.
11. Perozo, E., Cortes, D. M., and Cuello, L. G. (1999) *Science 285*, 73−78.
12. Jiang, Y., Lee, A., Chen, J., Cadene, M., Chait, B. T., and MacKinnon, R. (2002) *Nature 417*, 523−526.
13. Heginbotham, L., Lu, Z., Abramson, T., and MacKinnon, R. (1994) *Biophys. J. 66*, 1061−1067.
14. Splitt, H., Meuser, D., Borovok, I., Betzler, M., and Schrempf, H. (2000) *FEBS Lett. 472*, 83−87.
15. Anderson, J. A., Huprikar, S. S., Kochian, L. V., Lucas, W. J., and Gaber, R. F. (1992) *Proc. Natl. Acad. Sci. U.S.A. 89*, 3736−3740.
16. Sentenac, H., Bonneaud, N., Minet, M., Lacroute, F., Salmon, J. M., Gaymard, F., and Grignon, C. (1992) *Science 256*, 663−665.
17. Nakamura, R. L., Anderson, J. A., and Gaber, R. F. (1997) *J. Biol. Chem. 272*, 1011−1018.
18. Ou, X., Blount, P., Hoffman, R. J., and Kung, C. (1998) *Proc. Natl. Acad. Sci. U.S.A. 95*, 11471−11475.
19. Sukharev, S. I., Blount, P., Martinac, B., and Kung, C. (1997) *Annu. Rev. Physiol. 59*, 633−657.
20. Loukin, S. H., Vaillant, B., Zhou, X. L., Spalding, E. P., Kung, C., and Saimi, Y. (1997) *EMBO J. 16*, 4817−4825.
21. Minor, D. L., Jr., Masseling, S. J., Jan, Y. N., and Jan, L. Y. (1999) *Cell 96*, 879−891.
22. Sadja, R., Smadja, K., Alagem, N., and Reuveny, E. (2001) *Neuron 29*, 669−680.
23. Yi, B. A., Lin, Y. F., Jan, Y. N., and Jan, L. Y. (2001) *Neuron 29*, 657−667.
24. Epstein, W., Buurman, E., McLaggan, D., and Naprstek, J. (1993) *Biochem. Soc. Trans. 21*, 1006−1010.
25. Lu, Z., Klem, A. M., and Ramu, Y. (2001) *Nature 413*, 809−813.
26. Hackos, D. H., Chang, T. H., and Swartz, K. J. (2002) *J. Gen. Physiol. 119*, 521−532.
27. Matteson, D. R., and Swenson, R. P., Jr. (1986) *J. Gen. Physiol. 87*, 795−816.
28. Swenson, R. P., Jr., and Armstrong, C. M. (1981) *Nature 291*, 427−429.
29. Choe, H., Sackin, H., and Palmer, L. G. (1998) *J. Gen. Physiol. 112*, 433−446.
30. Choe, S., Stevens, C. F., and Sullivan, J. M. (1995) *Proc. Natl. Acad. Sci. U.S.A. 92*, 12046−12049.
31. Monks, S. A., Needleman, D. J., and Miller, C. (1999) *J. Gen. Physiol. 113*, 415−423.
32. Hong, K. H., and Miller, C. (2000) *J. Gen. Physiol. 115*, 51−58.
33. Collins, A., Chuang, H., Jan, Y. N., and Jan, L. Y. (1997) *Proc. Natl. Acad. Sci. U.S.A. 94*, 5456−5460.
34. Jiang, Y., Lee, A., Chen, J., Cadene, M., Chait, B. T., and MacKinnon, R. (2002) *Nature 417*, 515−522.
35. Holmgren, M., Shin, K. S., and Yellen, G. (1998) *Neuron 21*, 617−621.
36. Li-Smerin, Y., and Swartz, K. J. (2001) *J. Gen. Physiol. 117*, 205−218.
37. Li-Smerin, Y., Hackos, D. H., and Swartz, K. J. (2000) *J. Gen. Physiol. 115*, 33−50.

BI026393R